

NARAM 53: July, 2011

Team Division Entry for Research and Development

T-859 “What Could Possibly Go Wrong?”

Helicopter Duration Rotor-Blade Cross Sections:
Does Airfoil Matter?

A Comparison of a Conventional Cambered Airfoil
To Two Types of Rectangular, Non-Curved Cross Sections



MAA

Table of Contents

| | | |
|-------|---|----|
| I. | Overall Summary | 4 |
| II. | Glossary of Key Terms | 6 |
| III. | Background: How Does Autorotation Work? | 8 |
| IV. | A Plan to Compare Three Airfoils | 15 |
| V. | Methodology, Execution, and Results of Drop Tests | 19 |
| VI. | Conclusions | 29 |
| VII. | For Further Study | 30 |
| VIII. | Materials and Equipment / Costs | 31 |
| IX. | References | 32 |

NARAYAN 537-859-859

I. Overall Summary

There is a great deal of inherent complexity to the dynamical process known as autorotation. This study was undertaken with the goal of first clarifying how autorotation works and use this improved perspective to answer one of the oldest questions among those who have ever built a helicopter duration model: Does the airfoil of the rotor blade really matter? Can the choice of airfoil dramatically improve performance?

Perhaps surprisingly, there exist very few examples of any controlled empirical testing of helicopter duration performance. Reports by the Zunofark Team (1983) and DeMarco (2001) are notable exceptions, but this remains a remarkably untested landscape for empirical study. So we believe that even a limited series of drop tests could be a landmark in documenting autorotational performance.

We believe our results from testing and analysis presented in this report demonstrate very clearly that a cambered, flat-bottomed, curved-top airfoil can (and most likely will) outperform a flat plate of similar weight and material. In our first round of drop testing, it appears that despite being hampered by substantial drag and likely negative lift at the rotor tips, and despite a substantially lower rate of rotation, the cambered airfoil we tested significantly outperformed a flat plate of comparable weight and material. In a further round of follow up tests where we attempted to improve performance through increased tip angle of attack, the cambered airfoil dramatically outperformed the original flat plate tests. And we were unable to see a corresponding improvement with the flat blade when we increased tip angle of attack. While in no way can these tests be considered a comprehensive study of all possible configurations of the airfoils, we believe these results provide the first compelling empirical evidence for model rocketeers that a cambered airfoil will generally outperform a flat plate of similar weight and material, when flown under similar conditions.

We also conducted a secondary analysis of a type of airfoil that to our knowledge has never been previously considered for model rocketry. The “step-foil” is a counter-intuitive, rectangular airfoil than nonetheless did outperform a flat plate

in our initial round of tests, but failed to show improvement in our second round of tests where we increased tip angle of attack. So the step-foil may be a reasonable alternative for a modeler who does not wish to do all the work of creating a cambered airfoil but seeks better performance than would be obtained with a flat plate.

One of the most critical issues for the design of a helicopter duration model is the appropriate angle of attack at different points along the rotor blade. We discuss and explain in our report how a previous proposal by Van Milligan (1991) to optimize design by maintaining identical aerodynamic angle of attack for the entire rotor blade was based on a faulty assumption. So in looking ahead to the future of helicopter duration, there is considerable room for a further understanding about how to optimize the angle of attack, particular for the inner and middle portions of a rotor blade.

NARAYAN 537-807-8078

II. Glossary of Key Terms

Lift: Higher pressure below a wing (or rotor blade) than above it induces an upward force on that wing. We call this force lift, and it is caused by the flow of air over and under a given cross section of the wing, dependent on the wing's aerodynamic angle of attack and on the geometric shape (the "airfoil") of the wing's cross section. See also "camber" below.

Airfoil: For a lifting surface such as a wing or rotor blade, the particular geometric shape of a given cross section of that surface (considered relative to airflow).

Aerodynamic Angle of Attack: The angle of a cross section of a wing or rotor blade, measured in terms of the relative positions of leading edge, trailing edge, and the incoming airflow. The value of any given angle of attack is measured relative to "aerodynamic zero", which is the particular angle of attack resulting in zero lift for that particular wing's cross section. So the numeric value of the angle of attack depends on the particular airfoil of the wing's cross section.

Camber: A measure of asymmetry between the top and bottom geometries of a wing (or rotor blade) cross section. By definition, symmetric airfoils such as a flat plate have zero camber, while the typical flat-bottomed, curved-top airfoil will have positive camber. In general, camber affects where the aerodynamic zero line will be for any given cross section. Camber is generally correlated with both lift and drag, such that increasing camber may improve lift --- but this may be at the expense of higher drag. Also, large cambered airfoils may be more susceptible to laminar separation, a condition where airflow on top of the cross section becomes turbulent and "breaks away". Laminar separation may substantially reduce or curtail lift altogether.

Autorotation: Spin about a single axis, caused only by the flow of air across the rotating lifting surfaces (the rotor blades).

Helicopter Duration: Recovery of a model rocket such that the vertical descent is slowed by autorotation of the model about its vertical axis.

Flat plate: A symmetric airfoil with cross sections having a purely rectangular shape relative to the airflow.

C-foil: An abbreviation for “cambered airfoil”. This is a term used in this report to refer generically to positively cambered airfoils, particularly the flat-bottomed, curved-top variety that traditionally and commonly have been used by modelers. While there are infinitely many varieties of C-foils possible, we also use this term to refer specifically to one set of test blades we constructed for this study. Our tested C-foil was formed from 1/16 inch by 1 inch by 12 inch balsa strips with an airfoil shape roughly similar to that of an AG03 airfoil (approximately 6% thickness with camber = 2.0).

AG03 airfoil: One of a class of airfoils designed by Mark Drela, the AG03 is strictly flat-bottomed only for the aft portion, or trailing edge, of its underside. However, the thickness (6%) and camber (2.0) of the AG03 is very similar to the C-foil tested in our study, and so we considered the AG03 a useful reference for identifying theoretical properties that should be roughly similar to our tested C-foil.

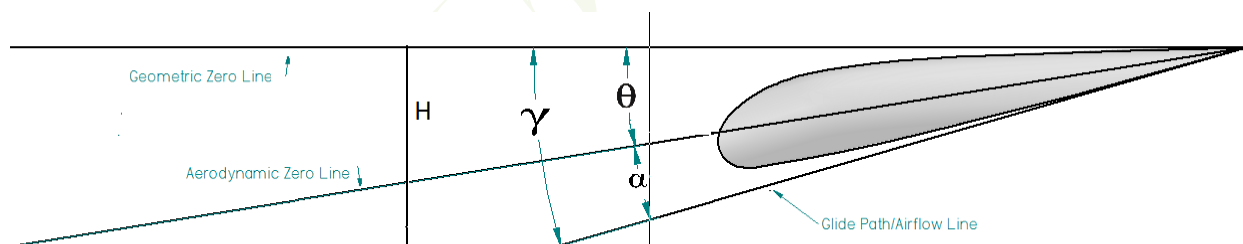
Step airfoil (“step-foil”): A particular airfoil constructed from two laminated flat plates, with the top plate having half the width of the bottom plate such that an asymmetry (and positive camber) is created. Air flowing above the top plate can be said to “step down” to the top of the lower plate, half way across the top of this airfoil. This is one particular type from the “Kline-Fogleman” class of airfoils, all of which involve one or more steps added above or below the cross section.

III. Background: How does autorotation work?

The phrase “helicopter duration” is typically used by rocketeers to refer to a method of slowing the vertical descent of a rocket using autorotation. In order for this to occur, the rocket typically must deploy lifting surfaces such that the flow of air over those surfaces induces sufficient autorotation to slow the model’s descent. The NAR Sporting Code includes a competition event based on achieving the longest duration flight using autorotation for recovery.

Whether for competition or recreational flying, helicopter duration is a challenging and complex process, with many factors affecting the performance of any particular model. The most common examples involve 3-4 rigid rotors, or blades, deployed upon the motor’s ejection charge so as to induce autorotation. Typically the blades must be set up with a particular angle of attack that will induce rotation. To understand how autorotation works, we must first understand the concept of the aerodynamic angle of attack of a lifting surface’s cross section relative to the direction of the airflow (See Figure 1).

Figure 1

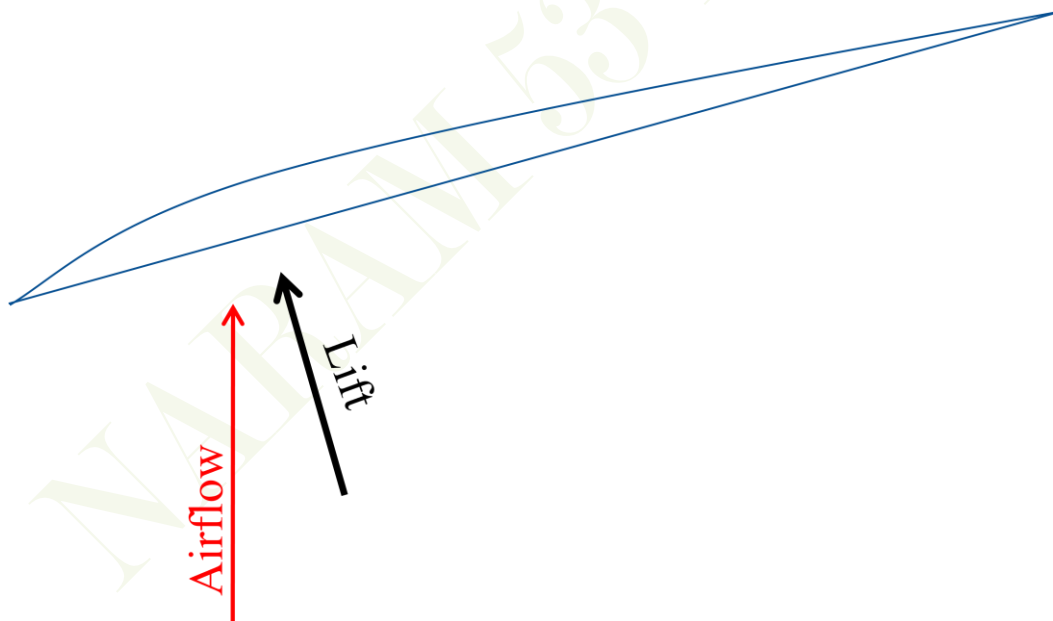


In Figure 1, the illustrated airfoil should be understood as one slice, or cross section, of one of the rotor blades. The Geometric Zero line can be thought of as parallel to the Earth’s surface below, so that the angle γ is measured from Geometric Zero down to the line of the airflow (of greater positive-valued magnitude the steeper the airflow). The angle γ can always be partitioned into

the sum of two angles ($\gamma = \Theta + \alpha$), where Θ can be thought of as the fixed incidence angle of the cross section of the blade, while α represents the aerodynamic angle of attack. The Aerodynamic Zero line is defined such that if the airflow were parallel with this line, zero lift would be produced by the particular cross section. As long as the airflow comes from below Aerodynamic Zero, then the angle of attack α has positive value and there is a lifting force associated with the cross section.

When the rotor blades are first deployed, the airflow line at that moment is essentially vertical, so that the angle γ is 90 degrees and alpha has a large positive value relative to the fixed value of Θ . Assuming Θ is positive, then at the moment of deployment the cross section of the blade produces a lifting vector force that is primarily upward but also somewhat in the direction of the leading edge of the blade, as shown in Figure 2. It is this “forward” component of the lifting force that starts the process of autorotation.

Figure 2



The next stage in the process of autorotation is the acceleration of the blades' spin, so that with increasing blade speed the airflow line tends closer to horizontal. At some point, the rotation will reach a maximum speed, with fixed angles γ and α (for any given cross section of the blade) such that the model as a whole will attain a constant rate of descent (defined in reference to Figure 1 as the lost vertical height H divided by the elapsed time t).

Note that in autorotational equilibrium, the actual geometric path traveled by any particular cross section of a rotor blade is analogous to a spring, or helix shape: The cross section is traveling in a circular path relative to the central axis of the rotor while simultaneously descending at a constant rate. But if we imagine this helix shape pulled into a straight line path, it would match the airflow line in Figure 2. Therefore, the airflow line is also referred to as the glide path for the particular cross section. For purposes of understanding the performance of the airfoil in terms of lift, drag, and rate of descent, the actual helical path of the cross section can be considered equivalent to a straight line path of a glider wing section, flying with glide angle γ , aerodynamic angle of attack α , at an incidence angle of Θ .

When a helicopter rotor model has reached autorotational equilibrium, this does not necessarily imply a constant rate of descent relative to the ground. We must always interpret this equilibrium as relative only to the immediate surrounding pocket of air. For example, this pocket of air may itself be a rising thermal relative to the ground, but we can still consider the model to be in equilibrium at a constant rate of descent relative to the immediate surrounding pocket of air.

However, even in autorotational equilibrium, the glide angle γ will be constant only for one particular cross section of the blade. For another cross section, say at a shorter distance from the central axis, the distance traveled along its helical path will be shorter, and therefore the glide angle γ associated with this more interior cross section will be larger. So γ necessarily differs across the length of the rotor blade, approaching 90 degrees for cross sections that are very close to the central axis of rotation. Furthermore, the velocity V of each cross section is

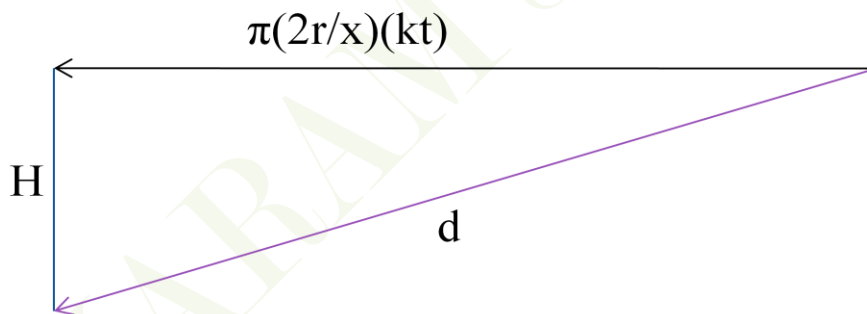
also different, since each cross section of one blade travels a unique distance within any fixed time t .

To determine the distance d traveled by a cross section of the blade along its helical path, we need only translate this problem successfully to an analogous “straight glide” framework. If we take r to be the length of the rotor blade, and then focus on a cross section that is $1/x$ of the rotor length from the central axis, first consider the distance traveled by this cross section if no height were lost: the distance traveled would simply be the circumference of the circle traced by the cross section, multiplied by the number of rotations in t seconds:

$$\text{Circumference} * (\# \text{ rotations}) = \pi(2r/x)(kt),$$

where k is the number of rotations per second and t is the number of seconds elapsed. If we “straighten” this distance out, it would be a geometrically flat line illustrated in Figure 3 as the top edge of an equilateral triangle. Then the true distance d traveled by the cross section in its helical path is the lower hypotenuse of the right triangle in Figure 3:

Figure 3



So the helical path distance d traveled by the cross section can be calculated using the Pythagorean formula:

$$d = (H^2 + [\pi(2r/x)(kt)]^2)^{0.5}.$$

And therefore, the velocity V for a cross section $1/x$ of the rotor length from the central axis is

$$V = (H^2 + [\pi(2r/x)(kt)]^2)^{0.5} / t.$$

So it is easy to see that the velocity of the blade is maximum for $x=1$ (the rotor tip cross section) and decreases for increasing values of $x>1$. Very near the central axis, V is approximately equal to H/t , which is also the general rate of descent, or “fall rate” f . A general formula for f is provided by Simons (1999):

$$f = (VD)/W = (V/W)(C_D S \rho V^2) / 2,$$

where D = Drag, W = weight, C_D = Drag coefficient, S = rotor area, and ρ = air density. One interesting aspect of this formula for descent rate is that, while both V and C_D vary with x , the product $C_D V^3$ must be constant because the descent rate applies to the whole model. This fact can in principle be used to derive $C_D V^3$ empirically from observations of the descent rate f .

This basic theoretical framework for understanding vertical autorotational descent (as illustrated by Figure 1 and quantified by the equation for the fall rate) was perhaps first formulated by Timothy Van Milligan (1991). Van Milligan’s NARAM 33 R&D entry sought a method for predicting the rate of descent of any given model as a function of the rotation rate k , assuming a constant angle of attack α . He sought to build upon a previous study by the Zunofark Team (1983) that a twisted blade (with varying Θ along the length of each rotor) is more effective at slowing the descent rate. Van Milligan embraced the Zunofark Team’s prescription and reasoned that the optimal “twist” for a blade would be one that maintained the same airfoil and a constant angle of attack α . The idea is that if an airfoil could be chosen for constant α such that C_L^3/C_D^2 is maximized, then the rate of descent will be minimized for the entire blade simultaneously. However, this “optimality criterion” to maximize C_L^3/C_D^2 is based on the assumption that weight is approximately equal to lift, or equivalently that γ has a very small value (Simons, 1999). The assumption is also equivalent to assuming H is very nearly zero and can be ignored. This assumption can be approximately true for a high performance glider where every cross section of the wing travels at

the same speed and at the same small glide angle γ . But this same assumption can never be reasonable for autorotational descent because the glide angle γ near the central axis necessarily approaches 90 degrees. So even if the glide angle γ at the rotor tip is close to zero, the optimality criterion (to maximize C_L^3/C_D^2) breaks down as we move inward from the rotor tip toward the central axis of rotation. Maximizing C_L^3/C_D^2 close to the rotor tips may contribute substantially toward optimizing autorotation for a slower descent, but it remains unclear exactly what criteria should be applied to designing the interior or middle portion of the rotor blade.

Exploring further what happens to the rotor tip's cross section, we might assume for a high performance rotor tip that H is close to zero, such that the velocity simplifies to

$$V = 2rk\pi \text{ (approximately).}$$

Therefore, the rate of descent is approximated by the formula

$$f = C_{D,\text{tip}} S \rho (2rk\pi)^3 / 2W \text{ (approximately),}$$

where $C_{D,\text{tip}}$ is the drag coefficient associated with the rotor tip. Empirical observation of the rotation rate k would then allow for an approximate calculation of $C_{D,\text{tip}}$. Later in this report, we evaluate observational data on f and k for certain test models and use these to derive estimates of $C_{D,\text{tip}}$ as well as $C_D V^3$ for those specific models.

Regarding the choice of airfoil, Bruce Markielewski's NARAM 42 R&D entry (2000) empirically tested and compared lift and drag for a flat-bottomed and curve-topped 1/16 inch thick balsa airfoil versus a 1/64 inch thick flat plate of plywood. His report is unique in focusing on (and calculating) the low Reynolds numbers for cross sections of a rotor blade at the typical velocities seen with small-model autorotation. His thesis was that due to the low Reynolds numbers associated with these low velocities, carefully formed and curved airfoils were unnecessary and did not add to performance. While Markielewski found lower drag and overall better lift-to-drag ratios associated with the 1/64 inch flat plate, it remains unclear whether this thin plywood blade would actually outperform the thicker

(yet possibly lighter) curved balsa blade in real-world flights. Presumably, the reduced drag of the small section of plywood tested seems unlikely to offset the disadvantages of the increased weight of a full model built with these rotors. And a 1/64 inch blade would presumably be too structurally weak if it were constructed of a lighter material such as balsa. Therefore, it's unclear whether Markielewski's conclusion can be generalized to say, a 1/16 inch balsa flat plate (which is more commonly the choice for 1/2A, A, or B motors).

In the next section, we discuss a study we performed to evaluate particular airfoils. It has been argued by some rocketeers (e.g. Barber, 2008) that it is unnecessary to use rotor blades with carefully formed airfoil shapes, and that a flat plate can perform as well as any other geometric shape. The Markielewski report has been used to support these claims, despite the fact that Markielewski compared blades of substantially different material and weight. We wanted to test the claim that a flat blade has equal or better performance, using controlled drop tests followed by a thorough examination of the data in the context of what is known theoretically about autorotational performance. Our research goal was to determine for small blades of roughly similar weight (all made of the most commonly used material, balsa) whether the airfoil really matters significantly.

IV. A Plan to Compare Three Airfoils

It has been a topic of debate for some time among competition modelers whether the type of airfoil on helicopter rotor blades really matters; some argue that a simple, rectangular flat plate (such as a rectangular cut of balsa wood) is sufficient and adequate to maximize performance, subject to other factors such as the twist of the blade to optimize angles of attack. Furthermore, the low Reynolds Numbers encountered during autorotation of small models raises questions about the effectiveness of cambered airfoils, such as whether cambered airfoils may have greater susceptibility to laminar separation during autorotation. Because the affect of the low Reynolds Numbers is complex and poorly understood, it is plausible that a flat plate for certain low Reynolds Numbers might equal or even outperform a cambered airfoil. These factors taken together strongly suggest that additional empirical and theoretical study is needed for modelers to more fully understand the benefits and limitations of cambered airfoils in this setting.

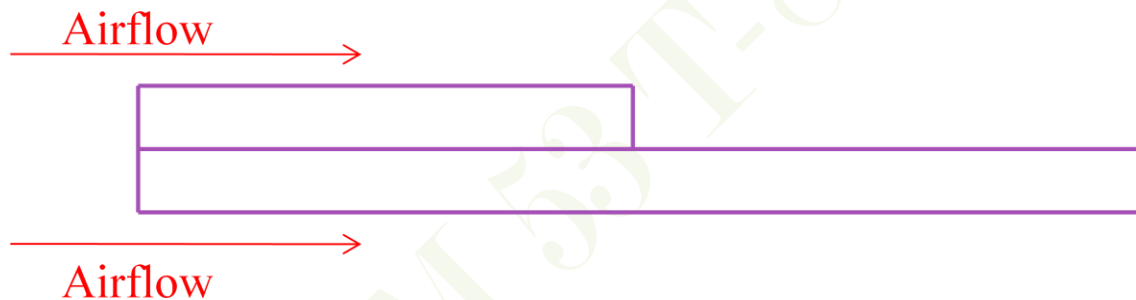
While it is not possible to do empirical testing of every conceivable combination of camber and angle of attack down the length of a rotor blade, we believe that some limited empirical testing can begin to shed better light on the fundamental question of whether a positively cambered airfoil (abbreviated below as “C-foil”) is worth the effort (usually requiring considerably greater time and work by the modeler to shape and sand the rotor blades appropriately). Perhaps surprisingly, there exist very few examples of any controlled empirical testing of helicopter duration performance. Reports by the Zunofark Team (1983) and DeMarco (2001) are notable exceptions, but this remains a remarkably untested landscape for empirical testing. So we believe that even our limited series of drop tests described below will be a landmark in documenting autorotational performance.

The two airfoils most commonly used by competition modelers are flat-bottomed C-foils and flat plates, most typically cut from 1/16 inch or 3/32 inch balsa. So 1/16 inch balsa is a natural choice for test rotors. We chose to do tests using a design typical for 1/2A or A HD: a 13 mm tube, 3 balsa fins, and three balsa rotors of approximate size 1/16 inch by 1 inch by 12 inches. Our primary comparison

would be between blades using a C-foil versus those with flat plate airfoil. Our tested C-foil was sanded to a shape roughly similar to that of an AG03 or similar type of airfoil (approximately 6% thickness, with camber approximately 2.0).

We decided to include in our testing a third type of airfoil which to our knowledge has not previously been considered for any model rocketry application. This type of airfoil is sometimes called a “step airfoil”, or just “step-foil”. The simplest way to create a step-foil is illustrated by Figure 4. This particular airfoil is constructed from two laminated flat plates, usually with the top plate having half the width of the bottom plate. As such, the step-foil is not a symmetrical airfoil --- It has a positive camber and therefore might plausibly be expected to increase lift relative to a flat plate.

Figure 4



Step-foils are part of a broader class of airfoils known as Kline-Fogleman airfoils, which may include multiple steps above or below the wing. In some other examples of Kline-Fogleman airfoils, the steps may be added to an otherwise curved airfoil shape.

Published research on Kline-Fogleman airfoils is predominantly negative, finding little or no benefit to many of the variations in step placement. But research specifically focused on top steps (such as that in Figure 4) does suggest better lift to drag ratios than that found with flat plates. For example, Nicolaides (1973) found a 44% increase in lift and a 30% improved lift-to-drag ratio over a flat plate using a step-foil similar to that illustrated in Figure 4. Lumsdaine and colleagues (1974) confirmed the findings of Nicolaides but found that other variations of Kline-Fogleman airfoils did not outperform the flat plate. The Lumsdaine paper is

intriguing because it focuses on potential applications to rotor blades, and although the primary focus of their paper is airfoils different from Figure 4, various comments within the paper regarding the Figure 4 type of airfoil suggest possible benefits that might be realized for helicopter duration models. For example, they noted that the step-foil may offer greater stability (less tendency to stall) at higher angles of attack, particularly at lower Reynolds numbers.

The Lumsdaine paper also comments on the leading theory for why step-foils increase lift: The theory is that a rotating vortex of air is created within the step that may accelerate the air flow on the upper side of the blade. This can be thought of as similar to why a golf ball with back spin produces lift: The back-spinning golf ball has an immediately close layer of air spinning in the direction of the back spin that accelerates airflow on top of the ball while slowing airflow below the ball. So as with the golf ball, lower pressure is created above the step-foil by more rapidly flowing air on top. This also explains why researchers have generally found the Kline-Fogleman airfoils with steps on the underside of the blade to be of no benefit.

Another theory we considered as relevant to small models is that the vortex of air within the step might resist tendencies for laminar separation associated with the low Reynolds Numbers we expect to see with small models. A key theoretical question is whether laminar separation is commonly a problem with rotor blades of a size and velocity similar to the ones in our test plan. So while we did not have any preliminary hypotheses regarding laminar separation, we nonetheless identified this as another possible benefit the step-foil might bring to helicopter duration models.

For these reasons, we chose to study the step-foil as an alternative airfoil to a flat plate. The step-foil would be similarly easy to construct and there exists enough published literature supporting the plausibility of a step-foil for autorotation of small models. Initially, we considered two versions of the step foil: One where each laminate layer was made from 1/16 inch balsa and a second step-foil where each layer was made from 1/32 inch balsa. After preliminary testing, the “dual 1/16” version was dropped from further consideration because it was just too

heavy (nearly double the weight) relative to the other blades studied. So the “dual 1/16” step-foil proved to be inconsistent with our goal of testing blade airfoils of an approximately similar weight. The remaining “dual 1/32” step-foil was actually the lightest of the three airfoils analyzed in this report, but all three types of blades were within one half gram of each other (between 4.6 and 5.1 grams per blade) so we did not see this difference as substantial. However, we noted that one potential benefit of the “dual 1/32” step-foil is that it might represent a slightly lighter blade that nonetheless should not be substantially weaker structurally.

Initial comparative tests of the three airfoils (described in detail in the next section) were planned using untwisted blades (i.e. Θ constant and α varying with x). While we acknowledge that untwisted blades are almost certainly not optimal, we wanted initial testing data collected on untwisted blades since these remain an easy-to-construct, popular choice of many modelers. Also, if there is a significant benefit in terms of lift to drag that is specific to one or two of these airfoils, presumably that relative benefit (due to airfoil alone) can be observed regardless of whether the absolute performance of any of the blades is optimized.

A second round of testing looked at the effect of the same airfoils but with an imposed twist (so Θ varied with x). The next section describes our testing methodology and execution in greater detail.

V. Methodology and Execution of Drop Tests

A single “base” model rocket was used for all drop tests; this model was designed and built to allow for modular rotor substitution. Rotors of each of the three types of airfoils tested were able to be attached at a constant 4-degree incidence to the hub of the base model, tested, and then removed from the base model so as to allow the next set of rotors to be attached at an identical incidence angle, etc. So each set of blades could be tested under the same controlled conditions. (Figure 5 below shows the base model with C-foil rotors attached).

Figure 5



The base model design was similar to George Gassaway’s 13mm Rotoroc. In order to ensure consistency of dihedral and the incidence angle Θ , as well as to

support the method of testing, three minor modifications to the Rotoroc were made. First, small balsa stops were added to the exterior of the body tube, instead of on the blades themselves, to ensure for consistency of the blade stops across the airfoil types. Second, the nose cone was removed and rubber band attachment S-hooks were externally attached around the body tube. Third, no motor or motor casing was installed. These last two modifications were performed to allow for a unique method of drop testing: The model would be dropped from a 25 foot, 8 inch height with rotors fully deployed, rotating around a taut string stretched vertically between the ground and a pole at the highest point (see Figure 6, below). So the central body tube for the base model needed to be kept as a smooth cylinder with no motor casing, nose cone, or any interior hooks or intrusions that might interfere with the autorotation about the string.

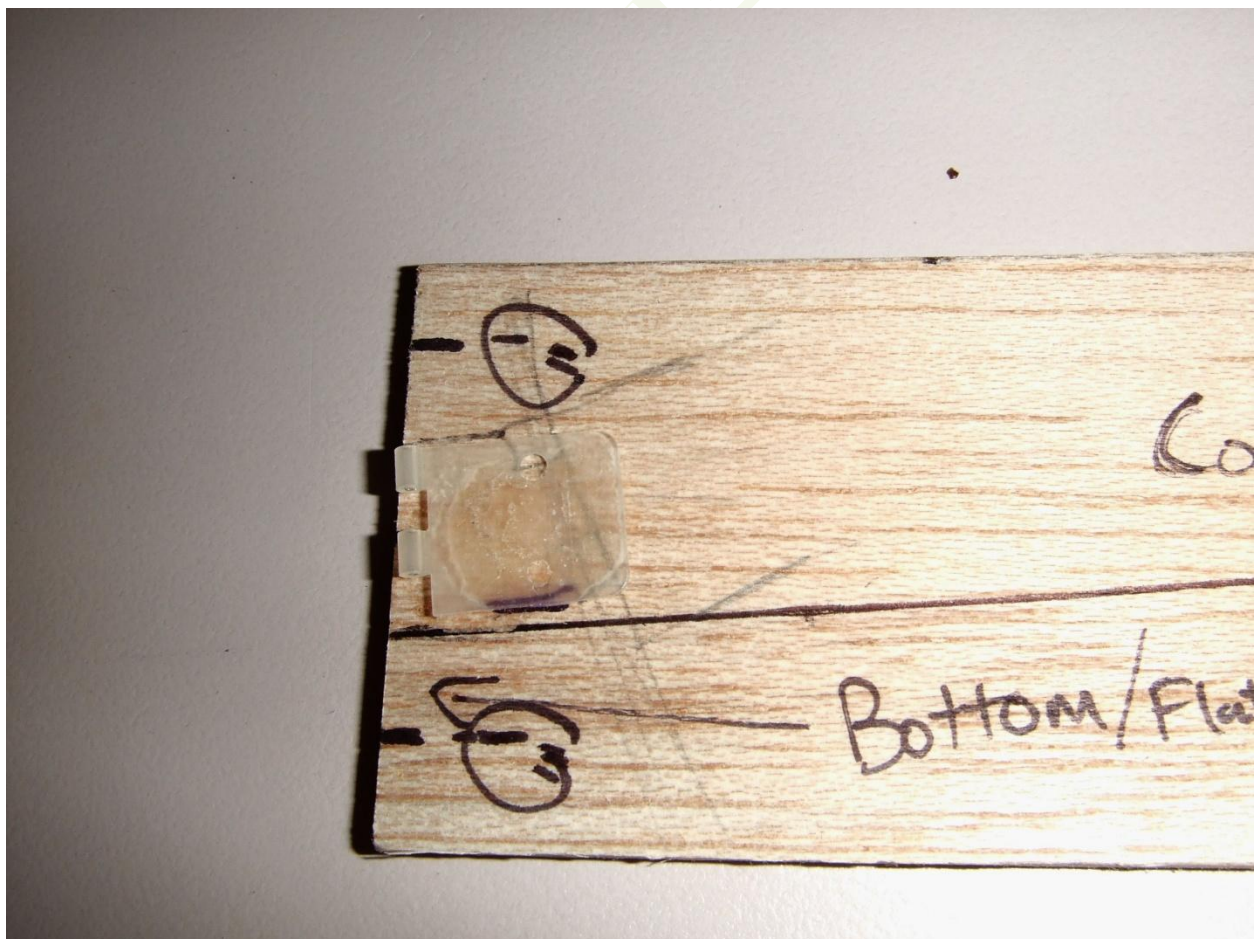
Figure 6



Although this “tether line” method of drop testing does not precisely match the real world flight of a helicopter duration model, it did greatly facilitate rapid testing and also controlled confounding variables that would have made extensive drop testing very challenging. For example, the tether line allowed for drop testing outdoors along the side of a building, where the lack of a tether line would likely have led to the model drifting randomly and perhaps getting lost or damaged. Having to recover the model after every drop would have tripled or quadrupled the amount of time needed to perform the roughly 80 drops we performed. With the model’s central tube on the tether line, this also reduced a potential source of random variability in duration due to horizontal drift.

Team member Chan Stevens developed a jig to allow for consistently reproducible placement of rotor blades onto a standardized hub (see Figure 7 below).

Figure 7



Fifty-two drop tests were conducted on June 25, 2011. Thirteen of these involved the “dual 1/16” step-foil blades and as such will not be discussed or presented herein. Results for the remaining 39 drop tests are provided in Table 1 on the next page. For the majority of drops, both team members timed the duration of the drop to the nearest hundredth of a second. In a few instances, a timer malfunction resulted in only one of the two times being captured. Also, for a small number of the drops high-speed video was recorded by the Team member on the ground, which necessitated in those instances that only the one other team member could time the drop. The average between the two timers was taken to be the official time for each drop.

By design, a total of 13 drops were completed for each of the sets. We anticipated a certain amount of random variation in the drop durations due to shifting pockets of air (thermal or sink). We planned to analyze by mean duration, expecting that random variability could be adequately controlled through the use of replicated drop tests. Thirteen replications of each drop was performed because the standard deviation for each set was anticipated to be about 1 second. In other words, we expected a range of roughly +/- 3 seconds about each airfoil's mean duration to be observed, with greater deviations either exceedingly rare or outliers caused by extreme thermal or sink. If 1 second is indeed the true standard deviation, then 13 replications per set would imply that the primary statistical comparison between the C-foil and the flat plate had an 80% chance of showing a statistically significant mean difference in duration, assuming the true difference was 1 second and using a one-sided 5% significance level.

Statistical results for the primary comparison between the C-foil and flat plate, as well as for the secondary comparison between the step-foil and the flat plate, are presented in Table 2. P-values shown are nominal and not adjusted for the dual statistical comparisons. Observed standard deviations were very close to 1 as expected, and both the C-foil and the step-foil showed statistically significant mean advantages over the flat plate of just under 1 second.

Table 1

| Airfoil | Blade Weight (grams) | Duration (seconds) |
|---|----------------------|--|
| <p>C-foil</p> <p>Maximum Rotation Rate = 2.01 rot/sec</p> | <p>4.9</p> | <p>6.215</p> <p>5.195</p> <p>8.93</p> <p>4.99</p> <p>6.71</p> <p>7.215</p> <p>6.325</p> <p>7.215</p> <p>6.715</p> <p>8.67</p> <p>7.925</p> <p>6.72</p> <p>7.12</p> |
| <p>Flat plate</p> <p>Maximum Rotation Rate = 2.67 rot/sec</p> | <p>5.1</p> | <p>7.115</p> <p>5.78</p> <p>4.16</p> <p>6.495</p> <p>6.625</p> <p>5.83</p> <p>7.06</p> <p>5.06</p> <p>5.055</p> <p>7.56</p> <p>5.25</p> <p>5.77</p> <p>6.5</p> |
| <p>Step-foil</p> <p>Maximum Rotation Rate = 2.50 rot/sec</p> | <p>4.6</p> | <p>5.305</p> <p>5.81</p> <p>5.9</p> <p>6.555</p> <p>7.155</p> <p>6.525</p> <p>8.48</p> <p>9.165</p> <p>6.615</p> <p>8.12</p> <p>7.235</p> <p>7.01</p> <p>6.75</p> |

Table 2

| Airfoil | Mean duration (sec) | Standard deviation | P-value* vs Flat Plate |
|------------|---------------------|--------------------|------------------------|
| Flat plate | 6.02 | 0.98 | |
| C-foil | 6.92 | 1.15 | 0.043 |
| Step-foil | 6.97 | 1.09 | 0.028 |

*P-values were unchanged if assuming either equal or unequal variances.

So these drop tests refute the claim that a flat plate will generally do as well or better than a C-foil. Intriguingly, the step-foil also outperformed the flat plate with duration very similar to the C-foil.

Video analyses allowed for us to calculate the maximum rate of rotation k for each of these blades, and these are presented as part of Table 1. Although the flat plate had the highest rotation rate, it performed the worst in terms of duration. So this illustrates how greater rotation rate does not necessarily imply greater lift and/or slower descent.

All video analyses performed from the June 25 and the later July 9 drop tests confirmed that a constant maximum rate of rotation was unique to each set of blades and could be replicated to a tenth of a second on repeated drops. There was considerable variation between drops in the amount of time it took to reach the maximum rotation speed, but not in the maximum rotation rate itself.

Table 3 presents the empirically calculated rates of descent, determined by dividing the 25.67 foot drop distance H by the mean durations from Table 2. Also included in Table 3 are the empirically derived values for $C_D V^3$ and the approximate tip values for V , $C_{D,tip}$, and the Reynolds Number.

Table 3

| Airfoil | Rate of descent (feet/sec) | $C_D V^3$ (feet/sec) ³ | Approx V at the tip ($2rk\pi$, in feet/sec) | Approx $C_{D,tip}$ | Reynolds Number at tip |
|------------|----------------------------|-----------------------------------|---|--------------------|------------------------|
| Flat plate | 4.26 | 71.3 | 16.8 | 0.015 | 9000 |
| C-foil | 3.71 | 62.3 | 12.6 | 0.031 | 7000 |
| Step-foil | 3.68 | 61.6 | 15.7 | 0.016 | 8000 |

* $C_D V^3$ was calculated assuming the rotor blades swept out an area of π feet², with the model weighing 1 ounce at an air density of 0.002378 slugs/foot³, corresponding to a mid-range temperature at sea level.

These calculations suggest that while the C-foil and the step-foil had a similar rate of descent, the C-foil had a higher drag coefficient at the tip (nearly double that of the step-foil and the flat plate). It is plausible that the C-foil provided substantially greater lift at the tip, compensating for the increased drag. One possible explanation for this is that the C-foil may have greater camber than both the flat plate and the step-foil, leading to a lower value for Θ than with the other two airfoils. So even though the geometric incidence angle of attachment was fixed for all three sets of blades, the aerodynamic angle of attack was probably in fact greater for the C-foil. This would explain both greater lift and greater drag being observed with the C-foil.

The Reynolds Numbers in the table were obtained by multiplying 6363 by the tip velocity, multiplied by 1/12 (the width of the rotor blades), then rounding that result to the nearest thousand. Using these values, we proceeded to consider some reference analyses using Profili software applied to Mark Drela's AG03 airfoil. The AG03 airfoil should be similar to the C-foil we tested (similar thickness, trailing edges, and camber). The Profili software allows for the calculation of drag and lift coefficients associated with particular Reynolds values and angles of attack. At a Reynolds of 7000, the software indicated that for a coefficient of drag for the AG03 to be in the neighborhood of 0.03, we were not maximizing the lift capability of the AG03. The lift coefficient at our observed level of drag was likely less than 0.1 and possibly even zero or negative. By contrast, at a Reynolds of 7000 Profili indicated that it is theoretically possible to achieve a lift coefficient as high as 0.7 with the AG03 at a much higher angle of attack.

So the implication of the analysis here is that, even though the C-foil outperformed the flat plate, it still did not appear to be anywhere near top performance. It is possible that the roughly 4-degree downward incidence angle for the whole blade resulted in an aerodynamic angle of attack for the C-foil tip of close to zero, possibly even negative valued. So we concluded that we should be able to improve the performance of the C-foil blade further by increasing the

angle of attack at the tip. One way to do this is to twist the blade so that α is increased at the tip.

A second round of testing was conducted on July 9, 2011 using altered blades with added rotor twist (to impart higher α at the tip). The balsa for each set of rotors was treated to allow for approximately zero geometric incidence at the tip for every blade but using the same hub incidence provided by the same base model for drop testing.

We expected to see results for all of the airfoils improve with the new round of testing, given that we were now using twisted rotors that should provide increased lift at the tips. We were surprised however to observe substantially worse performance for both the flat blades and the step-foils. The flat blades barely rotated at all, suggesting that too much drag had been introduced at the tips, possibly even a form of tip stall. We quickly gave up on completing a full set of replicated tests for the flat blades in this instance because their performance was so obviously terrible. It appeared that despite a likely lower aerodynamic angle of attack compared to the C-foil, the flat blade could not handle the increased attack angle. We acknowledged that possibly the flat blade would need reduced angle of attack near the hub combined with any increased angle at the tips. But since during the first round of testing the flat blades had spun at the fastest rotation rate among those tests, the implication is that even by coupling a higher tip angle with a lower hub angle, the flat blades appear unlikely to dramatically improve their descent rate.

By contrast, the C-foil adjusted for increased tip attack angle performed outstandingly, increasing its mean duration to 8.5 seconds while its maximum rotation speed shot up to 3.77 rotations per second. We confirmed the earlier results from the videotaping that showed that this maximum rotation speed was constant without substantial variability, regardless of the exact duration of the given drop test. The improved rotation speed and increased drop duration suggested that the tip cross sections on the first set of tests may have been in fact contributing negative lift, that the effective tip angle of attack was negative. This seems to be the only plausible explanation for how we could simultaneously and

dramatically increase lift (longer duration) while reducing drag (greater rotation speed), all from changing only the angle of attack at the outer portion of the blade. We needed to think in terms of why the first configuration with constant Θ had a retarded performance relative to these new tests, and the most plausible explanation is that the outer portion of the blade (the only thing different between the two sets of drop tests) was contributing substantially greater drag due to negative lift. Had the drag been due to positive lift, then a further increase in the tip angle of attack would have further slowed the rotation speed. So we conclude here that under the original drop test configuration, the C-foil tips were actually reducing lift, despite the fact that this C-foil blade still outperformed the flat blade. So evidently the original C-foil setup had provided sufficient lift to outperform the flat blade despite the fact that the outer portion of the blades was adding drag and reducing lift. When we corrected the C-foil's negative lift at the tips, the C-foil showed dramatically better performance in terms of slower descent rate (3.03 feet/sec), faster rotation speed (3.77), increased approximate velocity at the tip (23.7 feet/sec), and a substantially reduced approximate drag coefficient at the tip (0.004).

Similarly to the flat blade, the step-foil appears to have been unable to handle the increased angle of attack at the tip. This change clearly added enough drag to substantially slow the rotation rate and increase the descent rate by roughly a second and a half.

Table 4

| Airfoil | Mean Duration (sec) | Duration (seconds) |
|--|---------------------|---|
| <p>C-foil (increased tip AoA)</p> <p>Maximum Rotation rate = 3.77 rot/sec</p> | <p>8.48</p> | <p>11.89 6.02 9.025 7.47 7.465 6.055 6.58 7.96 8.25 13.06 9.9 9.85 6.66</p> |
| <p>Step-foil (increased tip AoA)</p> <p>Maximum Rotation rate = 1.52 rot/sec</p> | <p>5.60</p> | <p>7.135 4.575 5.52 4.72 8.22 8.31 4.345 6.28 5.53 4.12 4.33 4.78 4.97</p> |

VI. Conclusions

We commenced this study with the primary goal of evaluating whether or not airfoil matters in model rocket helicopter duration. And while there is a great deal of inherent complexity to the process of autorotation, we believe our analyses presented in this report demonstrate very clearly that a cambered airfoil can (and most likely will) outperform a flat plate of similar weight and material. In our first round of drop testing, it appears that despite being hampered by substantial drag and likely negative lift at the rotor tips, and despite a substantially lower rate of rotation, the C-foil outperformed the flat plate significantly. In our further round of follow up tests where we attempted to improve performance through increased tip angle of attack, the C-foil dramatically outperformed the original flat plate tests. We were unable to see a corresponding improvement with the flat blade when we increased tip angle of attack. While in no way can these tests be considered a comprehensive study of all possible configurations of the airfoils, we believe these results provide the first compelling empirical evidence for model rocketeers that a cambered airfoil will generally outperform a flat plate of similar weight and material, when flown under similar conditions.

Our secondary analysis was an exploration of a type of airfoil that appears never to have been previously tested in a model rocket. The “step-foil” did perform better than a flat plate in our tests, but failed to show improvement in our second round of tests where we increased tip angle of attack. So the step-foil may be a reasonable alternative for a modeler who does not wish to do all the work of creating a cambered airfoil but seeks better performance than would be obtained with a flat plate.

VII. For Further Study

One of the most critical issues for the design of a helicopter duration model is the appropriate angle of attack at different points along the rotor blade. We discussed in our report how a previous proposal by Van Milligan to maintain identical aerodynamic angle of attack for the entire rotor blade was based on a faulty assumption that may have applied to the rotor tip but not to the rest of the blade. So as both a theoretical and a practical question, it is unclear what strategy or criteria should be applied to optimize the angle of attack for the middle and inner portions of a rotor blade. Our study's evidence suggests that a twisted blade with varying incidence angle Θ can perform substantially better than a blade with fixed Θ , but this does not tell us what particular strategy for varying Θ is best. So there is room for a great deal of improvement in our understanding about this dynamical system.

VIII. Materials and Equipment / Costs

| | |
|---|---------|
| 13mm tubing for base rocket | \$1.00 |
| Balsa for rotors and fins | \$3.00 |
| Plastic hinges | \$5.00 |
| Gasoline for driving to location of test drops | \$20.00 |
| Other materials (string, tape, rubber bands, hooks, etc.) | \$0.50 |
| <hr/> | |
| | \$29.50 |

Multi-use Equipment that did not involve project-specific costs:

Profili aerodynamics computer software
Casio digital video camera
Digital stop-watches
Telescoping tubing (part of the drop testing setup)
Rulers and weight scales
Rotor jig

IX. References (in alphabetical order by author)

Barber, "Trip" (2008; NARCON presentation). Model Rocket Helicopter (Gyrocopter) Duration.

DeMarco, Alex (2001; NARAM 43 R&D entry). Free Spinning Hub versus Static Hub with Improvements on a Design.

Johnson, Wayne (1994). Helicopter Theory. Dover Publications, Inc. New York.

Langford, Ellis (2001; NARAM 43 R&D entry). Rotation! Optimization of Rotor Design for the Helicopter Duration Event.

Lumsdaine, E. et al (1974). An Investigation of Kline-Fogleman Airfoil Section for Rotor Blade Applications (Semi-annual report conducted for NASA).

Markielewski, Bruce (2000; NARAM 42 R&D entry). An Analysis of Helicopter Blade Section Design at Extremely Low Reynolds Numbers: Flat Plate versus Airfoil Shapes.

Nicolaidis, J.D. (April, 1973). Communication to Langley Research Center.

Simons, Martin (1999). Model Aircraft Aerodynamics. 4th Edition, Special Interest Model Books Ltd.

Van Milligan, Timothy (1991; NARAM 33 R&D entry). Calculating the Rate of Descent of a Helicopter Duration Rocket.

Zunofark Team (1983; NARAM 25 R&D entry). Rotor Twist on Rotoroc Models.



NARAWA